J Mater Sci (2009) 44:4661–4667
DOI 10.1007/s10853-009-3714-2

Synthesis of β-SiC nanostructures via the carbothermal reduction of resorcinol–formaldehyde/SiO_2 hybrid aerogels

Xintong Li · Xiaohong Chen · Huaihe Song

Received: 19 April 2009 / Accepted: 30 June 2009 / Published online: 16 July 2009

Abstract The novel resorcinol–formaldehyde/SiO_2 (RF/SiO_2) hybrid aerogels were chosen to synthesize the cubic silicon carbide (β-SiC) nanostructures via a carbothermal reduction route. In this process, the in situ polymerized RF/SiO_2 aerogels were used as both the silicon and carbon sources. The morphologies and structures of SiC nanostructures were characterized by X-ray diffraction (XRD), scanning electron microscope (SEM), and high-resolution transmission electron microscope (HRTEM) equipped with EDS. The effects of C/Si atomic ratios in RF/SiO_2 aerogels and heat treatment temperatures on the formation of SiC nanomaterials were investigated in detail. It was shown that β-SiC nanowhiskers with diameters of 50–150 nm and high crystallinity were obtained at the temperatures from 1400 to 1500 °C. The role of the interpenetrating network of RF/SiO_2 hybrid aerogels in the carbothermal reduction was discussed and a possible mechanism was proposed.

Introduction

Silicon carbide (SiC) shows many unique mechanical and thermal properties, such as high mechanical strength, high thermal conductivity, wide energy band gap, resistance toward oxidation, low thermal expansion coefficient, and excellent thermal stability [1], and therefore is considered as a promising material in many fields including biomaterials, high temperature semi-conducting devices [2], sorbent [3, 4], and membrane supports [5], and especially in catalysis [6–12] for many reactions in harsh environments. SiC has various crystalline phases including α-SiC (such as 6H–SiC and 4H–SiC) and β-SiC (3C–SiC, cubic form). Among these phases the β-SiC possesses the highest saturated electron drift velocity and is usually used as the preferred material for the high temperature, high power, and high frequency nanoelectronic devices [13]. As a result, the synthesis of β-SiC has attracted great attention all over the world for decades.

To date, various synthesis routes of β-SiC have been reported. For example, Sun et al. [14] prepared silicon carbide nanotubes and nanowires by the disproportionation of SiO using carbon nanotubes as both the template and the carbon source. Pitcher et al. [15] fabricated a smooth, continuous film of stoichiometric silicon carbide via the direct pyrolysis of polymethylsilyne. Hu et al. [13] synthesized nanocrystalline β-SiC from $SiCl_4$–Na–C system through a reduction–carbonization route. Shin et al. [16] utilized the carbothermal reduction of mineralized wood with silica at 1400 °C to synthesize SiC ceramics consisting of crystalline SiC nanoparticles as well as some whiskers. Pan et al. [17] succeeded in the preparation of oriented SiC nanowires via the reaction of aligned carbon nanotubes (as a template) with SiO at 1400 °C. Niu et al. [18, 19] synthesized SiC nanowires by a thermal evaporation of ferrocene or ZnS + carbon onto silicon wafers. Among the various synthesis methods, the sol–gel route has been a promising way to synthesize nanostructured SiC materials. Li et al. [20] prepared the SiC whiskers by the carbothermal reduction from aqua-mesophase and silica sol. Guo et al. [21, 22] have explored the sol–gel route to synthesize mesoporous SiC through the carbothermal reduction of tetraethoxysilane (TEOS)–phenolic resin-derived binary carbonaceous silicon xerogel containing nickel nitrate at 1250 °C. Hao et al. [23] synthesized

X. Li · X. Chen · H. Song (✉)
State Key Laboratory of Chemical Resource Engineering, Beijing University of Chemical Technology, Beijing 100029, People's Republic of China
e-mail: songhh@mail.buct.edu.cn

bamboo-like SiC nanofibers by the carbothermal reduction of the phenolic resin/silicon xerogel containing lanthanum nitrate. Zheng et al. [24] demonstrated the synthesis of mesoporous SiC via the carbothermal reduction reaction of saccharose-containing silicon xerogel at 1450 °C.

In this article, a sol–gel derived organic–inorganic hybrid aerogel, resorcinol–formaldehyde/SiO_2 (RF/SiO_2), was firstly employed as the precursor to synthesize β-SiC via the carbothermal reduction. In this study, the RF/SiO_2 hybrid aerogels were in situ formed by the co-polymerization of RF sol and SiO_2 sol and the subsequent supercritical drying. Aerogels are well-known to have high surface area and abundant open pores, which are advantageous for the mass transfer and the quick formation of SiC during the carbothermal reduction. In addition, this approach is a direct heat treatment process without any templates and catalysts for the aid of the preparation of β-SiC whiskers.

Experimental section

Preparation

All the reagents applied in this research are of analytical grade. The precursors, RF/SiO_2 hybrid aerogels, were prepared from RF sol and SiO_2 sol by the co-polymerization and the subsequent supercritical drying process. In a typical synthesis, firstly, 26.9 mL of TEOS, 28.0 mL of ethanol, 2.2 mL of water, and 0.96 mL of HCl (0.1 M) (to accelerate the hydrolysis of TEOS) were mixed together under magnetic stirring at 40 °C for 2 h to get the SiO_2 sol. Then 0.69 mL of ammonia ($NH_3{\cdot}H_2O$, 1 M) and 6.48 mL of water were added into the SiO_2 sol and maintained continuously by magnetic stirring for 10 min. The RF sol was synthesized as follows: 6.606 g of resorcinol (R) and 0.0636 g of sodium carbonate ($NaCO_3$) were dissolved in 10.8 g of water, followed by addition of 8.8 mL of 37% formaldehyde (F) under magnetic stirring at room temperature until the solution became light yellow. Further, by blending the prepared RF sol and SiO_2 sol under magnetic stirring at room temperature, a kind of hybrid sol was formed. The mixed sol was cured at 358 K for 72 h to form the wet hybrid gels. Then the obtained gels were dipped in acetone to exchange the containing water and dried by supercritical drying using petroleum ether as the extraction solvent ($T_c = 250$ °C, $P_c = 7$ MPa) for 2 h. Consequently, the dark red, transparent, and monolithic RF/SiO_2 hybrid aerogels were successfully obtained. The molar ratio of R:F:TEOS in this RF/SiO_2 was equal to 1:2:2, and thus the atomic ratio of C/Si in this precursor was 3, which actually accords with the desired stoichiometric ratio of C/Si when they are reacted into SiC as the following formula (I). In order to compare the effect of carbon content in the hybrid aerogels on the formation of SiC nanostructure, other RF/SiO_2 aerogels with the C/Si atomic ratios of 1 and 2 were also prepared, respectively.

$$SiO_2(s) + 3C(s) \rightarrow SiC(s) + 2CO(g) \quad \text{(I)}$$

Heat treatment and purification

The as-prepared hybrid aerogels were heated to 1200–1500 °C at the heating rate of 5 °C min^{-1} in a flow of argon gas and kept for 1–2 h at the final temperatures. Then the system was cooled down to room temperature at a rate of 5 °C min^{-1}. In order to remove the unreacted carbon and SiO_2, the as-prepared products were heated in air at 600 °C for 5 h and then were treated with a dilute mixture of nitric acid (65% HNO_3) and hydrofluoric acid (40% HF) (HNO_3/HF = 1:3, v/v) (Caution! This mixture is corrosive and hazardous!) for 72 h to get the purified SiC products. The yield of SiC was defined as the ratio of the amount of SiC formed to the theoretical amount deduced from complete conversion of carbon according to reaction (I). In addition, the RF/SiO_2 (C/Si = 3) was carbonized at 900 °C for 1 h to form C/SiO_2 composite in order to analyze the effect of the structure of the precursor on synthesis process.

Characterization

The X-ray diffraction (XRD) measurement was performed at a Rigaku D/max-2500B2+/PCX system using CuK_α radiation ($\lambda = 1.5406$ Å) over the range of 10–90° (2θ) at room temperature. Fourier transform infrared absorption (FTIR) was recorded on samples embedded in KBr pellets with a NICOLET NEXUS 870 FTIR spectrophotometer. The high-resolution scanning electron microscope (SEM) images of the products were obtained with a field-emission scanning electron microscope (FE-SEM, Hitachi S-4700) using an accelerating voltage of 20 kV. The transmission electron microscope (TEM) images were taken with a Hitachi-800 microscope. The high-resolution transmission microscope (HRTEM) images and EDS patterns were obtained with a JEOL JEM-3010 microscope equipped with EDS facilities. The samples for TEM and HRTEM observation were prepared by dispersing the products in ethanol with an ultrasonic bath for 10 min and a few drops of resulting suspension were placed on the copper grids. The nitrogen adsorption–desorption isotherms of the C/SiO_2 were determined at 77 K on a NOVA 4200e apparatus. Prior to the measurements, the sample was outgassed at 150° for 2 h. The BET specific surface area was calculated using the BET equation [25] for relative pressures in the range of $P/P_0 = 0.02$–0.2. The pore size distribution of the sample was determined from the desorption branch of

the hysteresis loop of the isotherm using the BJH formula with a cylindrical pore model [26].

Results and discussion

X-ray diffraction and FTIR spectrum

The effect of the concentration of the resorcinol (R) in the precursors on the yield of SiC was investigated. The yields of SiC synthesized from the precursors with C/Si atom ratio = 1, 2, and 3, namely, the molar ratio of R:TEOS = 1:6, 1:3, and 1:2, were 22, 69, and 80%, respectively. In other words, among the three precursors, the increase of the concentration of R can facilitate the carbothermal reduction process.

Figure 1 shows the XRD patterns of the 1500 °C heat-treated products from precursors with different C/Si atomic ratios. We can see clearly that the crystalline β-SiC was formed from the peaks at $2\theta = 35.6$, 41.4, 60.0, 71.7, and 75.4°, regardless of the C/Si atomic ratios in our research range. Meanwhile there are some impurities in the original products, especially as the C/Si atomic ratio is 1. From Fig. 1a it can be seen that crystalline SiO_2 peaks and some other weak peaks indexed to Al_2O_3 (from the aluminum boat) appeared, suggesting that the silicon source was excessive when C/Si atomic ratio was 1. As the C/Si atomic ratio increased from 1 to 3, the peaks of SiO_2 disappeared gradually and instead the peaks of β-SiC got much sharper. After air calcination and mixed-acid treatment, those peaks of impurities such as carbon, SiO_2 and Al_2O_3 almost disappeared (shown in Fig. 1d), and a single perfect β-SiC phase with high purity were found in the pattern with the reflection lines of (111), (200), (220), (311), and (222) planes of the crystalline blende structure β-SiC (space group *F-43m*(216)). A low-intensity peak at about $2\theta = 33.6°$ can be indexed to the stacking faults, which is marked with SF [27]. The refinement gave the cell constant of the product, $a = 4.3625$ Å calculated by the Bragg equation from the (200) diffraction plane of β-SiC ($2\theta \approx 41.4°$). Another important constant, the interplanar spacing of (111) d_{111} was also calculated from the XRD pattern to be 2.5224 Å. Both constants mentioned above are very close to the reported values of β-SiC ($a = 4.3589$ Å, $d_{111} = 2.5200$ Å) in the literature [28].

To analyze the purity of the SiC samples, further characterization of a representative SiC material prepared at 1500 °C for 2 h was made with FTIR. As seen in Fig. 2, an intense band at a frequency centered at 810 cm^{-1} indicates the transversal optic (TO) mode (Si–C stretching vibration) of β-SiC crystalline phase [29], and no trace of SiO_2 was detected in the spectrum. Combined with the XRD results, we can conclude that the Si–C structure was generated and the SiO_2 impurity was almost eliminated through purification.

SEM and TEM

The SEM images of a typical SiC product prepared at 1500 °C for 2 h before and after purification are shown in Fig. 3. It can be seen clearly that the sample consists mainly of whiskers with a diameter of 50–150 nm and a

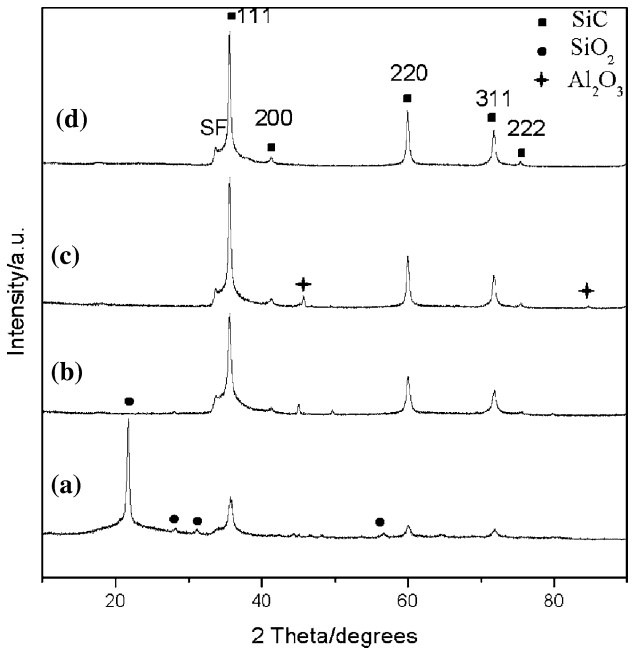

Fig. 1 X-ray powder diffraction patterns of the products treated at 1500 °C for 2 h from RF/SiO_2 hybrid aerogels with different C/Si atomic ratios: (*a*) C/Si = 1, (*b*) C/Si = 2, (*c*) C/Si = 3, and (*d*) C/Si = 3, (*a*, *b*, and *c* are the original (before purification) products, and *d* is the purified product)

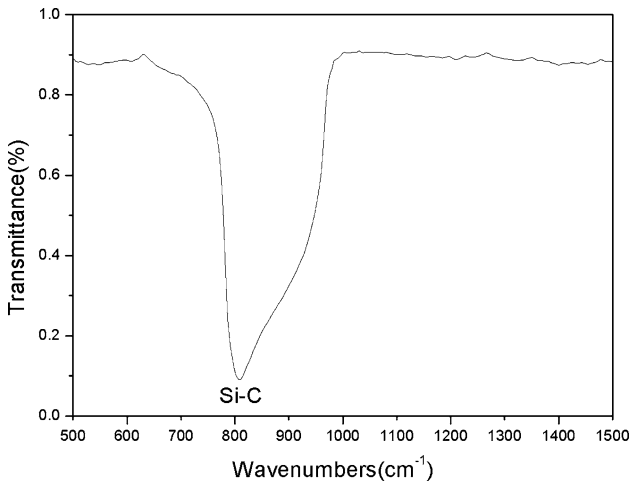

Fig. 2 FTIR spectrum of the purified SiC sample prepared at 1500°C for 2 h

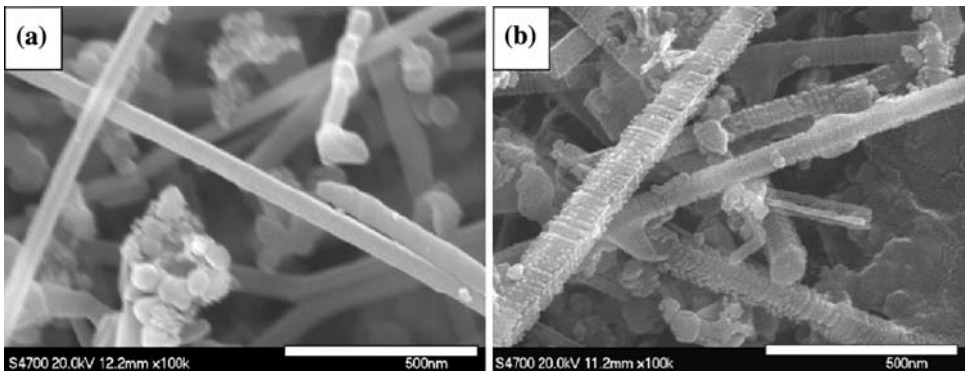

Fig. 3 SEM images of the product prepared at 1500 °C for 2 h before (**a**) and after (**b**) purification

length of several micrometers. The pristine SiC nanowhiskers hold a relatively smooth surface (Fig. 3a). After acid treatment, many ~10-nm thick platelets strung through the whiskers appeared (Fig. 3b) which can be ascribed to the etching effect of mixed acids. It was reported that the etching process by the mixture of HNO_3/HF was very selective to some parts of the whiskers [30]. When the whiskers were treated in the dilute mixture of HNO_3 and HF at room temperature, a slight amount of SiC on the surface was etched, making the stacking faults distinguishable.

Figure 4 shows the TEM images of the SiC product prepared at 1500 °C for 2 h. The observation (Fig. 4a) exhibits the morphology of nanowhiskers as well as some nanoparticles in the sample. The SAED pattern (the inset of Fig. 4a) suggests a single-crystalline β-SiC. The nanowhiskers have a diameter of ~100 nm and a length ranging from 500 nm to several microns. Figure 4b shows the HRTEM image of a single nanowhisker with a high density of planar defects, stacking faults perpendicular to the whisker axes which was reported in the previous literatures [17, 30]. The SiC nanowhisker shows a rough periphery, which is consistent with the SEM results. From Fig. 4c, we can see that the (111) fringes perpendicular to the axis are on average separated by 0.25 nm (marked with the parallel lines in Fig. 4c), which indicates that the single crystalline SiC nanowhiskers grow along the [111] direction. The EDS analysis (Fig. 4d) implies that the product is

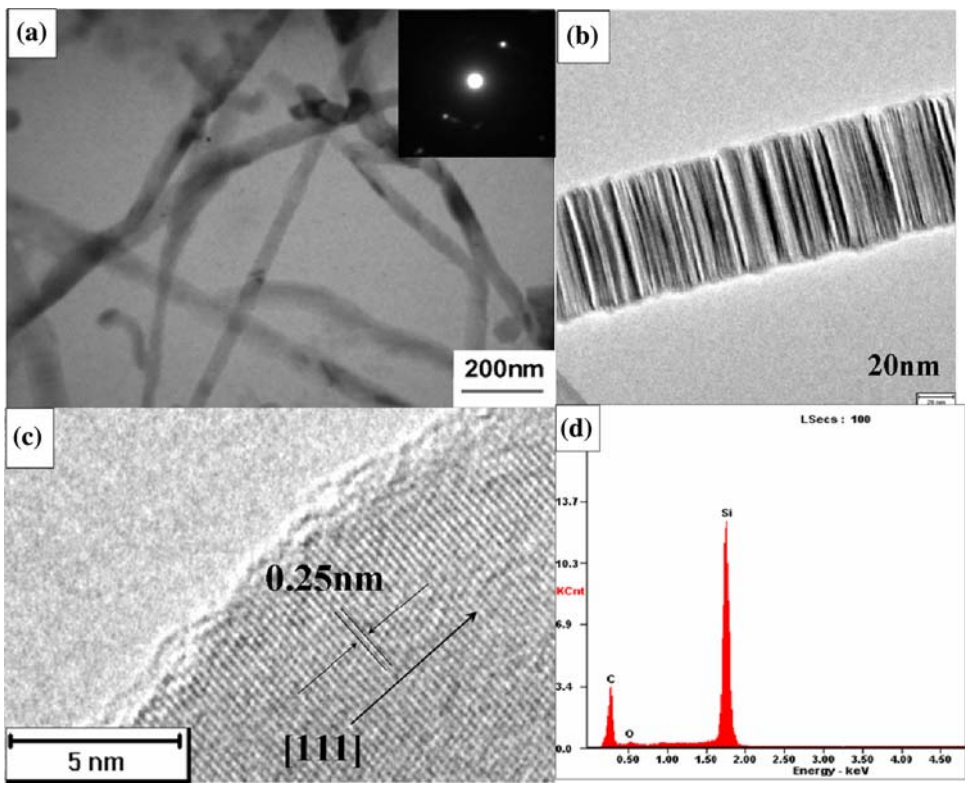

Fig. 4 **a** TEM image of the product prepared at 1500 °C for 2 h, (insets in **a**: corresponding SAED pattern), **b** HRTEM image of a β-SiC nanowhisker with stacking faults, **c** HRTEM image of the interplanar spacing of a single β-SiC nanowhisker, and **d** EDS spectrum taken from this product

almost composed of Si and C, which signifies the considerable purity of the sample. The weak peak of oxygen detected could be ascribed to the trace amount of residual silicon oxide even after mixed acids treatment.

Growth mechanism

In order to investigate the effects of carbothermal temperature on the formation of SiC, other temperatures were tried to synthesize SiC and the results are shown in Fig. 5. It can be seen that, when the heat treatment temperature was 1200 °C, the morphology of product was no obvious difference with that of the original RF/SiO_2 from the SEM observation, and the corresponding XRD pattern reveals that no SiC was formed at 1200 °C. At 1300 °C some "nano-beads" with the diameters in the range of 50–200 nm were found on the surface of product, and the main diffraction peaks of β-SiC (marked with dark square symbol) begin to appear in the XRD pattern, suggesting the possibility of SiC nuclei formation at this temperature. As the temperature reached 1400 °C, many β-SiC nanowhiskers with high crystallinity grew out from the RF/SiO_2 system. Combined with the results of 1500 °C in Figs. 1, 2, 3, and 4, it can be concluded that the suitable temperature for the large-area formation of β-SiC whisker is 1400–1500 °C in our RF/SiO_2 system.

Pore characteristics of the SiC precursor were also analyzed to study the effect of pore features on the formation of SiC. Figure 6 shows the nitrogen adsorption/desorption isotherm (at 77.3 K) and BJH pore size distribution (insets) of C/SiO_2 (900 °C carbonized-RF/SiO_2). It is found to own type-IV isotherms, reflecting the characteristics of mesoporous structure. From the analysis results, C/SiO_2 has a pore size distribution centered at 3.8 nm and a BET surface area of 250 m^2 g^{-1}. According to the previous study [31], the precursor, RF/SiO_2 hybrid aerogels, are

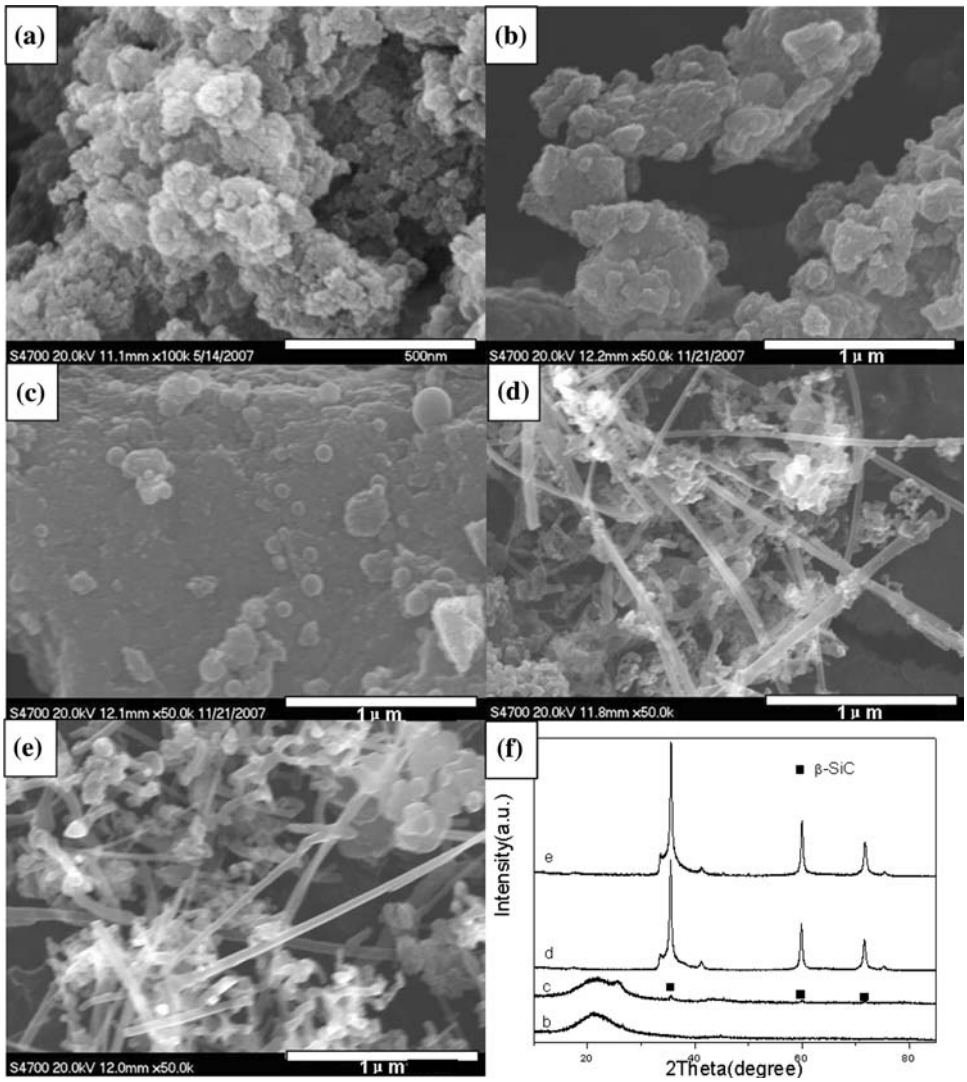

Fig. 5 SEM images and XRD patterns of the precursor and products synthesized at various different temperatures for 1 h (without purification): **a** original RF/SiO_2 hybrid aerogels and heat-treated products at, **b** 1200°, **c** 1300°, **d** 1400°, and **e** 1500°, respectively, and **f** XRD patterns of samples **b–e**

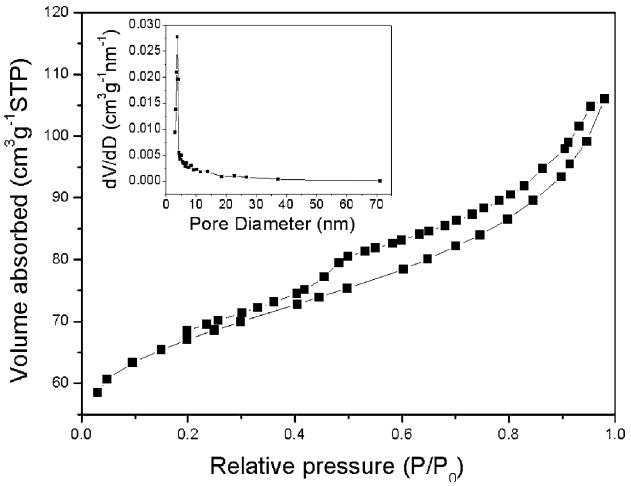

Fig. 6 Nitrogen adsorption/desorption isotherms (at 77.3 K) and BJH pore size distributions (insets) of C/SiO_2

constructed by a three-dimensional intercross framework of RF and SiO_2. These pore characteristics and homogeneous distribution of silica and carbon are undoubtedly to be favorable for the high contact of reactants and the mass transfer in the formation of pure SiC nanomaterials.

It is well-known that the synthesis of β-SiC via the carbothermal reduction of silica is a vapor–solid (V–S) growth process [20, 32], in which the suggested reactions listed below will take place. Firstly, SiO_2 component was reduced by carbon (carbon network from RF) to generate the gaseous components, SiO and CO (Reaction 1). CO, the product of the first step, can also react with SiO_2 to form gaseous SiO and CO_2 (Reaction 2). Then CO_2 reacted with the surrounding carbon network to produce CO according to Reaction 3. Finally the ultimate product, β-SiC, was obtained from the gaseous SiO, CO, and the carbon network through the Reactions 4 and 5. All these reactions can make a circle to continue the synthesis process from the starting steps.

$$SiO_2(s) + C(s) \rightarrow SiO(g) + CO(g) \quad (1)$$

$$SiO_2(s) + CO(g) \rightarrow SiO(g) + CO_2(g) \quad (2)$$

$$CO_2(g) + C(s) \rightarrow 2CO(g) \quad (3)$$

$$SiO(g) + 2C(s) \rightarrow SiC(s) + CO(g) \quad (4)$$

$$SiO(g) + 3CO(g) \rightarrow SiC(s) + 2CO_2(g) \quad (5)$$

The overall reaction is as follows:

$$SiO_2(s) + 3C(s) \rightarrow SiC(s) + 2CO(g) \quad (6)$$

A schematic illustration of SiC synthesis from the RF/SiO_2 hybrid aerogels is shown in Fig. 7. Firstly, SiC nucleated as "the growing seeds" on the surface of the precursor (Fig. 7a, b). As the SiC nuclei were formed, SiC nanowhiskers grew through gas–gas reaction between SiO and CO according to Reaction 5 (Fig. 7c, d). The interpenetrating pores could accelerate these reactions because those pores facilitate the diffusion of the formed gas products, such as SiO, CO, and CO_2. This suggests that, as the gaseous diffusion path, the interpenetrating pores play an important role in SiC synthesis process. As the reactions proceeded, the three-dimensional intercross framework of RF and SiO_2 would collapse; free space is then formed, allowing the gas–gas phase reaction (Reaction 5) to generate SiC nanowhiskers (Fig. 7e). As a result, the newly formed SiC did not inherit the pore structures of the precursors. Besides the SiC nanowhiskers, there are also particle-like SiC shown in Fig. 7e formed through the gas–solid reaction (Reaction 4).

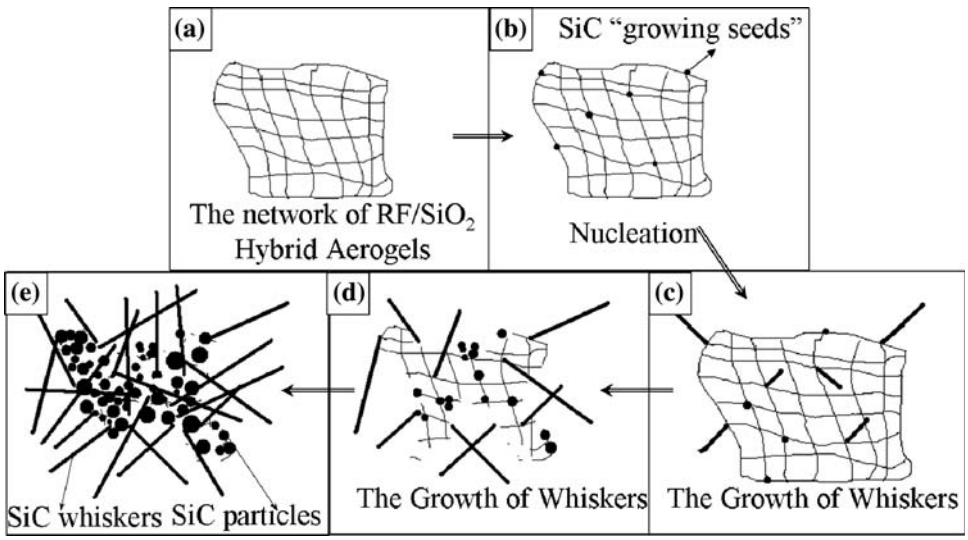

Fig. 7 Schematic illustration of SiC formation

Conclusion

β-SiC nanostructures with high purity and crystallinity were successfully synthesized by a carbothermal reduction using the novel RF/SiO_2 hybrid aerogels as the precursors. The prepared SiC nanowhiskers have diameters of 50–150 nm and lengths of several micrometers. The C/Si atomic ratio in the RF/SiO_2 hybrid aerogels and heat treatment temperature have great effects on the formation of SiC nanostructures. The interpenetrating networks in the RF/SiO_2 hybrid aerogels perform as the diffusion paths for the gaseous products and promote the efficiency of carbothermal reduction.

Acknowledgements This work was supported by the National Natural Science Foundation of China (50572003) and State Key Basic Research Program of China (2006CB9326022006).

References

1. Xi GC, Liu YK, Liu XY, Wang XQ, Qian YT (2006) J Phys Chem B 110:14172
2. Pol VG, Pol SV, Gedanken A (2005) Chem Mater 17:1797
3. Pham-Huu C, Estournes C, Heinrich B, Ledoux MJ (1998) J Chem Soc Faraday Trans 94:435
4. Pham-Huu C, Estournes C, Heinrich B, Ledoux MJ (1998) J Chem Soc Faraday Trans 94:443
5. Suwanmethanond V, Goo E, Liu PKT, Johnston G, Sahimi M, Tsotsis TT (2000) Ind Eng Chem Res 39:3264
6. Pham-Huu C, Gallo PD, Peschiera E, Ledoux MJ (1995) Appl Catal A 132:77
7. Moene R, Tijsen EPAM, Makkee M, Moulijn JA (1999) Appl Catal A 184:127
8. Moene R, Makkee M, Moulijn JA (1998) Appl Catal A 167:321
9. Keller N, Pham-Huu C, Crouzet C, Ledoux MJ, Savin-Poncet S, Nougayrede JB, Bousquet J (1992) Catal Today 53:535
10. Keller N, Pham-Huu C, Ledoux MJ (2001) Appl Catal A 217:205
11. Keller N, Pham-Huu C, Estournes C, Ledoux MJ (1999) Catal Lett 61:151
12. Shi YF, Meng Y, Chen DH, Cheng SJ, Chen P, Yang HF, Wan Y, Zhao DY (2006) Adv Funct Mater 16:561
13. Hu JQ, Lu QY, Tang KB, Qian YT, Zhou GE, Liu XM, Wu JX (1999) Chem Mater 11:2369
14. Sun XH, Li CP, Wong WK, Wong NB, Lee CS, Lee ST, Teo BK (2002) J Am Chem Soc 124:14464
15. Pitcher MW, Joray SJ, Bianconi PA (2004) Adv Mater 16:706
16. Shin YS, Wang CM, Exarhos GL (2005) Adv Mater 17:73
17. Pan ZW, Lai HL, Au FCK, Duan XF, Zhou WY, Shi WS, Wang N, Lee CS, Wong NB, Lee ST, Xie SS (2000) Adv Mater 12:1186
18. Niu JJ, Wang JN (2007) Eur J Inorg Chem 25:4006
19. Niu JJ, Wang JN (2007) J Phys Chem B 111:4368
20. Li XK, Liu L, Zhang YX, Ling LC, Shen SD, Ge S (2001) Carbon 39:159
21. Jin GQ, Guo XY (2003) Microporous Mesoporous Mater 60:207
22. Guo XY, Jin GQ (2005) J Mater Sci 40:1301. doi:10.1007/s10853-005-6957-6
23. Hao YJ, Jin GQ, Han XD, Guo XY (2006) Mater Lett 60:1334
24. Zheng Y, Zheng Y, Lin LX, Ni J, Wei KM (2006) Scr Mater 55:883
25. Brunauer S, Emmett PH, Teller E (1938) J Am Chem Soc 60:309
26. Barrett EP, Joyner LG, Halenda PP (1951) J Am Chem Soc 73:373
27. Koumoto K, Takeda S, Pai CH, Sato T, Yanagida H (1989) J Am Ceram Soc 72:1985
28. Joint Committee on Powder Diffraction Standards (JCPDS) 29-1129
29. Liao LS, Bao XM, Yang ZF, Min NB (1995) Appl Phys Lett 66:2382
30. Cambaz GZ, Yushin GN, Gogotsi Y, Lutsenko VG (2006) Nano Lett 6:548
31. Chen XH, Yang SX, Song HH (2006) Adv Mater Res 11–12:619
32. Yao JF, Wang HT, Zhang XY, Zhu W, Wei JP, Cheng YB (2007) J Phys Chem C 111:636